

Supplementary Information

1. Concentrations of iron in different water types

Supplementary Table 1 documents published concentrations of iron measured across a range of different glacial water types. We draw upon these published concentrations to constrain the likely iron concentrations in Antarctic subglacial meltwaters (SGM-Fe, here defined as aqueous, nanoparticulate iron species and some colloids $< 0.4 \mu\text{m}$ following (Raiswell and Canfield, 2012)). The reported range of Fe concentrations, which includes values for Greenland runoff and valley glaciers in the McMurdo Dry Valleys Antarctica and groundwaters present in glacial sediments, leads us to assume lower and upper values for concentrations (including colloids in some cases) of 3 and 30 μM respectively derived from the range of iron concentrations reported in runoff from valley glaciers in the McMurdo Dry Valleys/Greenland Ice Sheet runoff and groundwaters present in glacial sediments respectively. Fluxes of DFe in subglacial meltwater are calculated from the product of these concentration values and the total water flux (52.8 Gt a^{-1} : see main manuscript).

Supplementary Table 1 Summary of iron concentrations measured in glacier ice, sea ice, glacial runoff and groundwaters worldwide (mean, range or single sample concentrations reported)

Sample/site description	Reference	Concentration (μM)	Filtration method
Iceberg/glacier ice			
Iceberg, Antarctica	(Raiswell et al., 2008)	0.00069	0.2 μm filters
Glacier ice, Antarctica	(Raiswell et al., 2008)	0.0015	0.2 μm filters
Glacier ice, Antarctica	(Loscher et al., 1997)	0.0204	0.4 μm filters
Sea ice/snow on sea ice			
Snow (on sea ice), Antarctica	(Loscher et al., 1997)	0.042	0.4 μm filters
Sea ice, Antarctica	(Loscher et al., 1997)	0.019	0.4 μm filters
Sea ice, Antarctica	(Martin et al., 1990)	0.026	No filtration/acid digest – total dissolvable Fe
Glacial runoff, Northern Hemisphere			
Greenland Ice Sheet runoff	(Statham et al., 2008)	0.053	0.4 μm filters
Greenland Ice Sheet runoff	(Bhatia et al., 2013)	2-9	0.2 μm filters
Glacial runoff, Antarctica			
Runoff - Blood Falls, McMurdo Dry Valleys, Antarctica	(Mikucki et al., 2009)	3450	0.2 μm filters
Runoff - Onyx River at Lower Wright glacier margin, McMurdo Dry Valleys, Antarctica	(Green et al., 2005)	1.1	0.4 μm filters
Runoff - streams in McMurdo Dry Valleys, Antarctica (Onyx river and Vanda station)	(Sheppard et al., 1997)	2.1	0.4 μm filters
Glacial groundwaters			
Groundwaters in glacial drift aquifers, Nebraska, USA	(Gosselin et al., 2001)	35.5	0.45 μm filters
Groundwaters in glacial drift aquifers, S. Michigan, USA	(Kim et al., 2002)	18.4	0.45 μm filters
Groundwaters in glacial drift aquifers, Michigan, USA	(Szramek et al., 2004)	17100	0.45 μm filters
Groundwaters in glacial drift aquifers, Illinois, USA	(Warner, 2001)	31.5	0.45 μm filters

2. Antarctic meltwater export

2.1. Evidence for meltwater export

There is mounting evidence that meltwater generated at the bed of the Antarctic Ice Sheet is exported to the Southern Ocean (SO) from the ice sheet margin. Land-based and sub-marine geomorphological data display paleo-channels and other hydrological features indicative of the occurrence of outburst floods (Sugden et al., 2006; Lowe and Anderson, 2003), which is also supported by direct observations of such flood events from the ice margin (Goodwin, 1988). Traces of channels incised into the base of a large number of ice shelves around the continent have also been recently observed in satellite images of the ice shelf surface and suggests extensive meltwater export at the ice sheet margins by large subglacial channels (Le Brocq et al., submitted). Continuous discharge of water from the ice sheet is also supported by sand and/clay deposits in ice-marginal core records which indicate that sediment-laden meltwater plumes originate beneath the ice sheet (Lowe and Anderson, 2002). Sub-marine groundwater discharge has also recently been measured from the East Antarctic coast, at rates that were two orders of magnitude higher than rates reported for mid latitude sites (Uemura et al., 2011). Hence, the notion that meltwater generated at the bed of the ice sheet is ultimately exported is now becoming well established.

3. Numerical modeling

3.1. Description of the MIT global ocean biogeochemical/ecological model

We employ the MIT global ocean biogeochemical/ecological model (Monteiro et al., 2010) which combines the $1^\circ \times 1^\circ$ MITgcm ocean model with a self-assembling phytoplankton ecosystem (Follows et al., 2007). The ocean circulation is prescribed from the ECCO-GODDAE state estimate in which the model circulation has been constrained to closely match observations (Wunsch and Heimbach, 2007). The phytoplankton ecosystem is self-assembled from a random population of 78 phytoplankton including different types of diatoms, nitrogen fixers, *Prochlorococcus*, other small cyanobacteria and large eukaryotes (Follows et al., 2007; Monteiro et al., 2010). The model also includes two zooplankton types (large and small). In addition to the activity of phytoplankton and grazing, the model captures the dynamics of dissolved and particulate organic matter. Biogeochemical cycles of nitrogen, phosphorus, iron and silica are resolved within the MIT global ocean model.

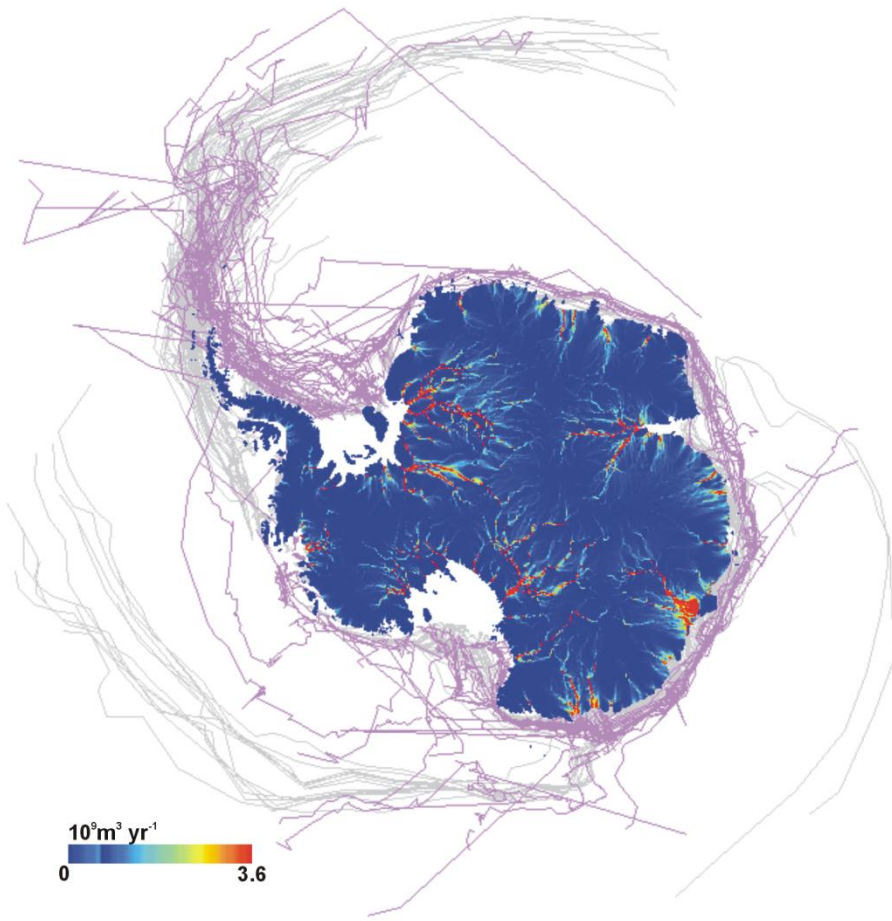
Within the model framework, geochemical and biological processes interact via the uptake of nutrients, phytoplankton growth and decay and remineralisation of organic matter at depth. The four main nutrient cycles of phosphorus, nitrogen, silica, and iron are all represented in the model. Of particular interest to this study is the manner in which the model deals with iron cycling and how the surface ocean phytoplankton community simulated by the model respond to changes in iron bioavailability. The

parameterisation of the iron cycle within the MIT model is prescribed (Parekh et al., 2004; Parekh et al., 2005), with iron existing in a ‘free’ state or complexed to an organic ligand with binding strength of K_{FeL} ($2 \times 10^5 \mu M^{-1}$). The amount of iron that exists in an organic complex is determined by the total number of ligands available (where the maximum ligand concentration = 1 nM) and the stability of the ligand complex (K_{FeL}). Removal of iron occurs either via biological uptake or by scavenging of free iron to particles, with a scavenging rate of $1.1 \times 10^{-3} d^{-1}$. The rate at which iron is removed from the surface ocean waters and transported to depth is controlled by the sinking rate of particulate organic matter (POM) ($10 m d^{-1}$). The rate at which dissolved iron is returned to the water column through remineralisation depends on whether it is in an organic or nanoparticulate form. The organic matter remineralisation rate is $0.01 d^{-1}$, while the particulate matter rate is $0.02 d^{-1}$. Therefore, the vertical profile of dissolved iron in the water column is determined by the balance between the rate of iron acquisition and mineralization versus the rate of iron losses via biological uptake and/or scavenging. Finally, iron sources from subglacial meltwaters and icebergs are prescribed as a forcing into the surface of the ocean.

3.2 Iron input fluxes to the model: comparison with observations

Five model scenarios are simulated, each prescribing a different set of iron inputs. These scenarios are A) Dust-only, B) Dust+iceberg fluxes C) Dust+subglacial meltwater (where $[Fe] = 3 \mu M$) and D) Dust+subglacial meltwater (where $[Fe] = 30 \mu M$) (S Table 1) and E) Dust+icebergs+subglacial meltwater fluxes (where $[Fe] = 3 \mu M$). The following sections detail how iron fluxes from a) dust, b) subglacial meltwater and c) icebergs are calculated and input to the model as forcing fields for primary productivity of the Southern Ocean. The four types of iron source inputs to the model are described in the following sections. Other glacially-sourced nutrient inputs (e.g Si) are not included in these scenarios.

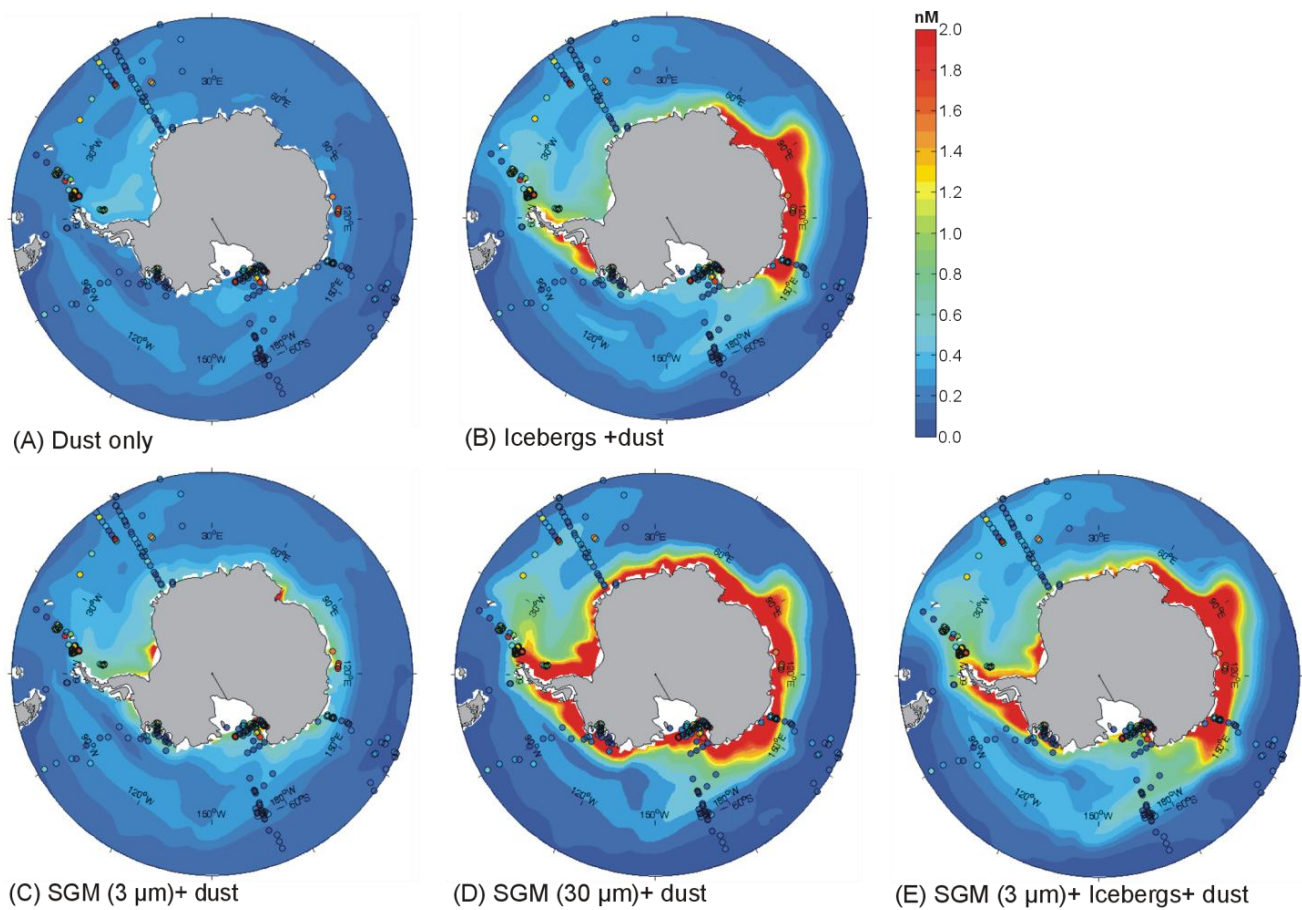
The modelled iceberg tracks are comparative to observations (Suppl. Fig. 1). The general trend is for decay in the concentration of iceberg tracks with distance from the ice sheet. The strong Antarctic Coastal Current flowing anti –clockwise around the continent pins the icebergs to the near coastal zone. In agreement with observational data there are three locations where icebergs are able to escape northwards; (1) tracking up the Antarctic Peninsula ($\sim 55^\circ W$), (2) around the Kergulen Plateau ($\sim 85^\circ E$) and (3) in the Ross Sea ($\sim 180^\circ E$). In these regions the bathymetry of the ocean floor drives the ocean currents northwards so transporting the icebergs entrained within them away from the continent (Gladstone et al., 2001). Once the icebergs move northwards they are caught in the Antarctic Circumpolar Current, which carries them clockwise into the sub-polar waters of the Southern Ocean.



Supplementary Figure 1. Observed iceberg tracks for icebergs greater than 10 nautical miles (pink) compared to the modelled iceberg tracks (grey). Meltwater generation beneath the ice sheet is also shown using a coloured scale (in $10^9 \text{ m}^3 \text{ yr}^{-1}$ – see legend).

The iron input scenarios described in the main manuscript provide the MIT model with four different iron input fields, resulting in the surface ocean iron concentrations shown in Suppl. Fig. 2. These modelled surface (0-100 m vertically integrated) iron concentrations are compared with measurements of surface dissolved iron (0-103 m) in the Southern Ocean from a recent compilation of data (Moore and Braucher, 2008) (superimposed on the model results in Fig. 2). Measured dissolved iron concentrations in open water areas from the Southern Ocean tend to be $< 0.2 \text{ nM}$ which agrees largely with the modelled values of all four scenarios. Enhanced coastal dissolved Fe concentrations ($> 2 \text{nM}$) are evident in simulations B-E, consistent with marine observations from the Antarctic marginal ice zone, where observed Fe concentrations of up to and greater than 1 nM have been observed (Sedwick et al., 2000; Gerringa et al., 2012; Ardelan et al., 2010; Westerlund and Ohman, 1991). Elevated iron concentrations measured in

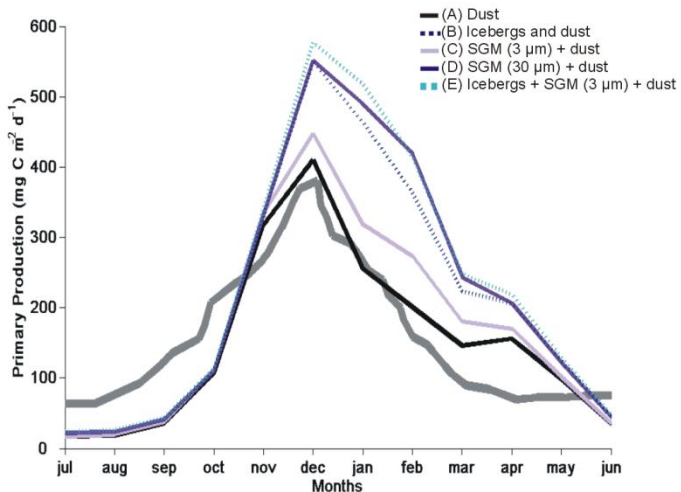
coastal polynyas around Pine Island Glacier have been shown to be capable of sustaining phytoplankton growth, up to 150 km away from the glacier front (Gerringa et al., 2012). In this study the authors assigned the iron input as due to the melt out of basal sediments beneath the Pine Island Glacier tongue, where this iron-rich meltwater is laterally advected within ocean currents to supply the phytoplankton blooms. Studies that sample waters surrounding icebergs have also found increased dissolved iron concentrations ($> 2 \text{ nM}$) in waters up to several kilometers distance from melting bergs (Lin et al., 2011). Such elevated ocean surface iron concentrations are not apparent in the control dust-only model simulations (A) and point towards an additional source of Fe near the continent. Previously identified sources of this additional Fe are sea-ice, coastal upwelling, coastal sediments, and, more recently, icebergs (Lancelot et al., 2009). Hence our model results indicate that additional glacially-derived iron fluxes are likely to have a significant impact on the coastal concentrations of iron.



Supplementary Figure 2 Model-data comparison of dissolved iron concentrations in the surface waters of the Southern Ocean. Model results are in color and data are represented by the dots (based on the data compilation of (Tagliabue et al., 2012)). Modelled dissolved iron concentrations in the surface waters of the Southern Ocean under Scenarios A-E.

3.2 Modelling the annual cycle of Southern Ocean Primary Productivity

The temporal pattern of PP simulated in all model runs corresponds well with that derived from satellite data (Arrigo et al., 2008), with peak productivity in the austral summer (Supplementary Figure 3).



Supplementary Figure 3 Monthly time series of modelled annual primary productivity for aeolian dust, icebergs and subglacial meltwater (SMW) and a comparison with the modelled primary productivity previously documented by ref (Arrigo et al., 2008) (thick grey line).

Supplementary references

Ardelan, M. V., Holm-Hansen, O., Hewes, C. D., Reiss, C. S., Silva, N. S., Dulaiova, H., Steinnes, E., and Sakshaug, E.: Natural iron enrichment around the Antarctic Peninsula in the Southern Ocean, Biogeosciences, 7, 11-25, 2010.

Arrigo, K. R., van Dijken, G. L., and Bushinsky, S.: Primary production in the Southern Ocean, 1997-2006, J. Geophys. Res., 113, C08004, 10.1029/2007jc004551, 2008.

Bhatia, M. P., Kujawinski, E. B., Das, S. B., Breier, C. F., Henderson, P. B., and Charette, M. A.: Greenland meltwater as a significant and potentially bioavailable source of iron to the ocean, Nature Geosci., 6, 274-278, 10.1038/ngeo1746

<http://www.nature.com/ngeo/journal/v6/n4/abs/ngeo1746.html#supplementary-information>, 2013.

Follows, M. J., Dutkiewicz, S., Grant, S., and Chisholm, S. W.: Emergent Biogeography of Microbial Communities in a Model Ocean, Science, 315, 1843-1846, 10.1126/science.1138544, 2007.

Gerringa, L. J. A., Alderkamp, A. C., Laan, P., Thuroczy, C. E., De Baar, H. J. W., Mills, M. M., van Dijken, G. L., van Haren, H., and Arrigo, K. R.: Iron from melting glaciers fuels the phytoplankton blooms in Amundsen Sea (Southern Ocean): Iron biogeochemistry, *Deep-Sea Res Pt II*, 71-76, 16-31, DOI 10.1016/j.dsr2.2012.03.007, 2012.

Gladstone, R. M., Bigg, G. R., and Nicholls, K. W.: Iceberg trajectory modeling and meltwater injection in the Southern Ocean, *J Geophys Res-Oceans*, 106, 19903-19915, 2001.

Goodwin, I. D.: The nature and origin of a jokulhlaup near Casy Station, Antarctica, *J Glaciol*, 34, 95-101, 1988.

Gosselin, D. C., Harvey, F. E., and Frost, C. D.: Geochemical Evolution of Ground Water in the Great Plains (Dakota) Aquifer of Nebraska: Implications for the Management of a Regional Aquifer System, *Ground Water*, 39, 98-108, 10.1111/j.1745-6584.2001.tb00355.x, 2001.

Green, W. J., Stage, B. R., Preston, A., Wagers, S., Shacat, J., and Newell, S.: Geochemical processes in the Onyx River, Wright Valley, Antarctica: Major ions, nutrients, trace metals, *Geochim Cosmochim Ac*, 69, 839-850, 2005.

Kim, M.-J., Nriagu, J., and Haack, S.: Arsenic species and chemistry in groundwater of southeast Michigan, *Environmental Pollution*, 120, 379-390, 2002.

Lancelot, C., de Montety, A., Goosse, H., Becquevort, S., Schoemann, V., Pasquer, B., and Vancoppenolle, M.: Spatial distribution of the iron supply to phytoplankton in the Southern Ocean: a model study, *Biogeosciences*, 6, 2861-2878, 2009.

Le Brocq, A. M., Ross, N., Griggs, J., Bingham, R. G., Corr, H., Ferraccioli, F., Jenkins, A., Jordan, T. A., Payne, A., Rippin, D., and Siegert, M.: Ice shelves record channelised water flow beneath the Antarctic Ice Sheet, *Nature:Geoscience*, submitted.

Lin, H., Rauschenberg, S., Hexel, C. R., Shaw, T. J., and Twining, B. S.: Free-drifting icebergs as sources of iron to the Weddell Sea, *Deep Sea Research Part II: Topical Studies in Oceanography*, 58, 1392-1406, 2011.

Loscher, B. M., De Baar, H. J. W., De Jong, J. T. M., Veth, C., and Dehairs, F.: The distribution of Fe in the antarctic circumpolar current, *Deep Sea Research Part II: Topical Studies in Oceanography*, 44, 143-187, 1997.

Lowe, A., and Anderson, J.: Evidence for abundant subglacial meltwater beneath the paleo-ice sheet in Pine Island Bay, Antarctica, *J Glaciol*, 49, 125-138, 2003.

Lowe, A. L., and Anderson, J. B.: Reconstruction of the West Antarctic ice sheet in Pine Island Bay during the Last Glacial Maximum and its subsequent retreat history, *Quaternary Sci Rev*, 21, 1879-1897, 2002.

Martin, J. H., Gordon, R. M., and Fitzwater, S. E.: Iron in Antarctic Waters, *Nature*, 345, 156-158, 1990.

Mikucki, J. A., Pearson, A., Johnston, D. T., Turchyn, A. V., Farquhar, J., Schrag, D. P., Anbar, A. D., Priscu, J. C., and Lee, P. A.: A Contemporary Microbially Maintained Subglacial Ferrous "Ocean", *Science*, 324, 397-400, DOI 10.1126/science.1167350, 2009.

Monteiro, F. M., Follows, M. J., and Dutkiewicz, S.: Distribution of diverse nitrogen fixers in the global ocean, *Global Biogeochem. Cycles*, 24, GB3017, 10.1029/2009gb003731, 2010.

Moore, J. K., and Braucher, O.: Sedimentary and mineral dust sources of dissolved iron to the world ocean, *Biogeosciences*, 5, 631-656, 2008.

Parekh, P., Follows, M. J., and Boyle, E.: Modeling the global ocean iron cycle, *Global Biogeochem Cy*, 18, Artn Gb1002

Doi 10.1029/2003gb002061, 2004.

Parekh, P., Follows, M. J., and Boyle, E. A.: Decoupling of iron and phosphate in the global ocean, *Global Biogeochem Cy*, 19, Artn Gb2020

Doi 10.1029/2004gb002280, 2005.

Raiswell, R., Benning, L. G., Tranter, M., and Tulaczyk, S.: Bioavailable iron in the Southern Ocean: the significance of the iceberg conveyor belt, *Geochem T*, 9, -, Artn 7

Doi 10.1186/1467-4866-9-7, 2008.

Raiswell, R., and Canfield, D.: The iron biogeochemical cycle Past and Present, *Geochemical Perspectives*, 1, 1-220, 2012.

Sedwick, P. N., DiTullio, G. R., and Mackey, D. J.: Iron and manganese in the Ross Sea, Antarctica: Seasonal iron limitation in Antarctic shelf waters, *J Geophys Res-Oceans*, 105, 11321-11336, 2000.

Sheppard, D. S., Deely, J. M., and Edgerley, W. H. L.: Heavy metal content of meltwaters from the Ross Dependency, Antarctica, *New Zealand Journal of Marine and Freshwater Research*, 31, 313-325, 10.1080/00288330.1997.9516769, 1997.

Statham, P. J., Skidmore, M., and Tranter, M.: Inputs of glacially derived dissolved and colloidal iron to the coastal ocean and implications for primary productivity, *Global Biogeochem Cy*, 22, -, Artn Gb3013

Doi 10.1029/2007gb003106, 2008.

Sugden, D. E., Bentley, M. J., and Ó Cofaigh, C.: Geological and geomorphological insights into Antarctic ice sheet evolution, *Philosophical Transactions of the Royal Society A: Mathematical, Physical and Engineering Sciences*, 364, 1607-1625, 10.1098/rsta.2006.1791, 2006.

Szramek, K., Walter, L. M., and McCall, P.: Arsenic mobility in groundwater/surface water systems in carbonate-rich Pleistocene glacial drift aquifers (Michigan), *Applied Geochemistry*, 19, 1137-1155, 2004.

Tagliabue, A., Mtshali, T., Aumont, O., Bowie, A. R., Klunder, M. B., Roychoudhury, A. N., and Swart, S.: A global compilation of dissolved iron measurements: focus on distributions and processes in the Southern Ocean, *Biogeosciences*, 9, 2333-2349, DOI 10.5194/bg-9-2333-2012, 2012.

Uemura, T., Taniguchi, M., and Shibuya, K.: Submarine groundwater discharge in Lützow-Holm Bay, Antarctica, *Geophys. Res. Lett.*, 38, L08402, 10.1029/2010gl046394, 2011.

Warner, K. L.: Arsenic in Glacial Drift Aquifers and the Implication for Drinking Water—Lower Illinois River Basin, *Ground Water*, 39, 433-442, 10.1111/j.1745-6584.2001.tb02327.x, 2001.

Westerlund, S., and Ohman, P.: Iron in the Water Column of the Weddell Sea, *Mar Chem*, 35, 199-217, 1991.

Wunsch, C., and Heimbach, P.: Practical global oceanic state estimation, *Physica D*, 230, 197-208, DOI 10.1016/j.physd.2006.09.040, 2007.